Woody breast myopathy broiler show age-dependent adaptive differential gene expression in *Pectoralis major* and altered *in-vivo* triglyceride kinetics in adipogenic tissues

Pramir Maharjan,[*] Antonio Beitia,[†] Jordan Weil,[*] Nawin Suesuttajit,[*] Katie Hilton,[*] Justina Caldas,[‡] Cole Umberson,[*] Diego Martinez,[*] Byungwhi Kong,[*] Casey M. Owens,[*] and Craig Coon[*,1]

[*] *Department of Poultry Science, Center of Excellence for Poultry Science, University of Arkansas, Fayetteville, AR 72701, USA;* [†] *Aviagen Group. Huntsville, AL 35806, USA; and* [‡] *Cobb Vantress, Inc. Siloam Springs, AR 72761, USA*

ABSTRACT A study was conducted to understand the differentially expressed genes in *Pectoralis (P) major* under woody breast (**WB**) myopathy condition in a high yielding broiler strain using RNA-sequencing at the growing (d 21) and finishing (d 42 and d 56) grow-out ages. Follow-up study was conducted to understand the in vivo triglyceride (**TG**) synthesis (d 49) occurring in adipogenic tissues using deuterium oxide (^2H_2O) as a metabolic tracer. Results indicated the top physiological systems affected in myopathy broiler were related to the musculoskeletal system (d 21, 42, and 56) and cardiovascular system (d 42 and 56). Ubiquitin-specific proteases are expressed higher in myopathy broiler at d 21 (OTUD1) and d 42 (SACS) that potentially indicated higher degradation of muscle protein occurring at those ages. While genes related to transcription factors and muscle cell differentiation (ZNF234, BTG2) and muscle growth (IGF1) were upregulated with myopathy broiler suggesting concurrent muscle fiber regeneration. The downregulation of PYGB and MGAM genes related to carbohydrate transport and metabolism at d 42 potentially indicated nutrient-deficient state of myopathy affected fibers; whereas the nutrient-deficient physiological state of cells seemed to be counteracted by up-regulation of genes related to carbohydrate (ALDOB, GPD1L2) at d 56. There was a reduced ($P < 0.05$) in vivo TG synthesis in liver of the myopathy broiler (0.123 %/hr) compared to non-myopathy broiler (0.197 %/hr). The majority of TG synthesized in liver with myopathy broiler could conceivably be delivered to *P. major* (rather than to abdominal fat pad storage) to fulfil the increased energy need of muscle cells (via TG lipolysis and fatty acid [**FA**] oxidation). The increased utilization of FAs in the WB affected muscle could result in reduced secretion of FAs into blood circulation leading to sub-optimal availability of FAs for re-esterification for TG synthesis in liver. Results indicated that myopathy broiler at later age (d 56) of grow-out period were synchronously going through adaptive physiological processes of feedback responses to adverse cellular states.

Key words: pectoralis major, woody breast myopathy, gene expression, TG kinetics, physiological adaptation

2021 Poultry Science :101092
https://doi.org/10.1016/j.psj.2021.101092

INTRODUCTION

The broiler meat market has evolved over the years with increasing selection pressure shifted towards attaining greater meat yield for increased cut-up parts such as breast and thighs (Kuttappan et al., 2016). Selection for quantitative traits such as breast yield and growth rate exert physiological pressure which can alter typical myocellular gene expression pattern and associated pathways bringing antemortem histological and biochemical alterations in muscle tissues (Abasht et al., 2016; Maharjan et al., 2019; Maharjan et al., 2020a; Soglia et al., 2019; Mutryn et al., 2015). The pathophysiological changes in muscle tissue of high yielding broiler lines have resulted in the emergence of several muscle myopathies including one called woody breast (**WB**) myopathy. The WB myopathy condition affects the *Pectoralis (P) major* (poultry breast muscle) of broiler (Bailey et al., 2015; Kuttappan et al., 2016). A recent study reported WB myopathy incidence of ~9% for 10,483 filets evaluated in high breast meat yielding strain from a flock which produced larger broiler (2.72 kg−4.53 kg) (Wold et al., 2017). The WB affected filet is

Received October 14, 2020.
Accepted March 4, 2021.

[1]Corresponding author: ccoon@uark.edu

phenotypically stiff and visually unappealing along with reduced protein quality. Histologically, it has been reported to exhibit moderate to severe polyphasic myodegeneration with variable degrees of interstitial connective tissue accretion or fibrosis (Sihvo et al., 2014).

The etiopathology to the WB phenotype is unknown. Many studies have been conducted particularly over the past 5-year span to understand the associated pathophysiological processes in WB myopathy condition (Velleman and Clark, 2015; Maharjan et al., 2019, 2020a,b,c; Kuttappan et al., 2017).Woody breast affected birds are phenotypically detected by palpation of the breast area (Kuttappan et al., 2016). The direct palpation of the breast muscle is a detection technique that is qualitative and can only be detected post manifestation of the myopathy condition. The early detection of WB myopathy condition in a growing broiler would require molecular signatures and proper identification of physiological biomarkers. A timeline transcriptomic analysis could give a proper evaluation of the preceding pathophysiological phenomena that WB myopathy broiler could be undergoing as the broiler is growing and manifesting this myopathy condition. Previous metabolomics and transcriptomic studies with WB myopathy broiler reported the involvement of cardiovascular system and dysregulated lipid (Maharjan et al., 2019; Papah and Abasht, 2019). The present study attempts to understand the differentially expressed (**DE**) genes in *Pectoralis (P) major* under WB myopathy condition using RNA-sequencing at the earlier and later phases of a broiler grow-out period and forecasts the possible molecular and physiological pathways that could be involved as underlying etiopathogenesis for WB myopathy condition. The next objective of present study was to gain a better understanding of in vivo lipogenesis (triglyceride (TG) synthesis) occurring in adipogenic tissues of myopathy broiler using deuterium oxide (^2H_2O) as a metabolic tracer. The use of labelled water or ^2H_2O to understand TG synthesis for poultry is a new technique as of the authors' knowledge. In vivo TG synthesis may provide insight into the ongoing differential lipid metabolism in broiler with increased WB myopathy compared to broiler with less myopathy manifestation.

METHODS

Broiler Type, Husbandry, and Sampling

Strain B, a high yielding broiler strain, reported in Maharjan et al., (2020c) was utilized in the present study for transcriptomic evaluations. The performance parameters (weight gain, FCR, yield), protein turnover, and collagen turnover of Strain B associated with this study can be retrieved from Maharjan et al., (2020c). Furthermore, Strain B was reported to be myopathy vulnerable strain. Birds utilized in the study were reared utilizing the recommended primary breeder nutrition for the strain and the husbandry guidelines followed were approved by Institutional Animal and Care and Use Committee protocol #17080.

Tissue Sample Selection for RNA Sequencing (RNA-Seq)

Tissue samples collected (antero-ventral region of *P. major*) from the Maharjan et al. (2020c) were utilized for the RNA-Seq studies. Tissue samples were initially subjected to histological staining by Masson Trichrome staining and microscopic analysis for the gross lesions to differentiate myopathy-affected tissue (Calvi et al., 2012). The criteria used for the differentiating the WB affected tissue from non-affected tissue were based on the presence of gross lesions such as degenerating and regenerating muscle fibers leading to various shape and sizes and massive deposition of collagen in perimysial and endomysial spaces occurring in affected muscle tissue (Maharjan et al., 2020b). Three age groups- d 21, 42, and d 56 were selected for the present study to cover the early and finishing broiler grow-out phases. The sample differentiation was WB score 1 for d 21 and WB score $>$ 2 for d 42 and d 56 versus non-affected tissue (WB score $=$0) at each age group. The WB myopathy score were measure in the scale of 0−3, 0 being the non-myopathy broiler and 3 being the severely affected myopathy broiler (Tijare et al., 2016). A total of 5 different samples were subjected for RNA-Seq analysis for each age group and each category of myopathy broiler and non-myopathy broiler.

Tissue Processing for RNA Isolation and Sequencing

The collected *P. major* tissue samples were processed for RNA extraction using Zymo Quick RNA Miniprep kit (Cat. No. R1054). First, 50 mg of tissue was excised and lysed following the procedures of Zymo protocol. A DNase step was incorporated to remove gDNA. The quality and concentration was respectively determined after the RNA extractions using HS RNA Tapestation and HS RNA Qubit (Agilent Tech, Santa Clara, CA). 200 ng of RNA with a RNA integrity number (RIN) higher than 7 was used for each RNA-Seq library. Libraries were constructed using the Nugen Universal Plus mRNA Library Prep Kit (Part No. 0520-A01) (Redwood City, CA), then loaded at 1.5pM and sequenced with a RealSeq Biosciences (Santa Cruz, CA, USA). Single End 75nt reads and dual 6nt indexes were carried out for sequencing.

RNA-Seq Data Analysis

The data were further processed through filtering, trimming, QC, alignments, count matrix generation, and then subjected to DE. The DE genes were calculated using the DESeq2 package in R (Liao et al., 2019; R Core Team, 2019). The adjusted P-value cut off was set at $\leq$ 0.05 for identifying the significant genes

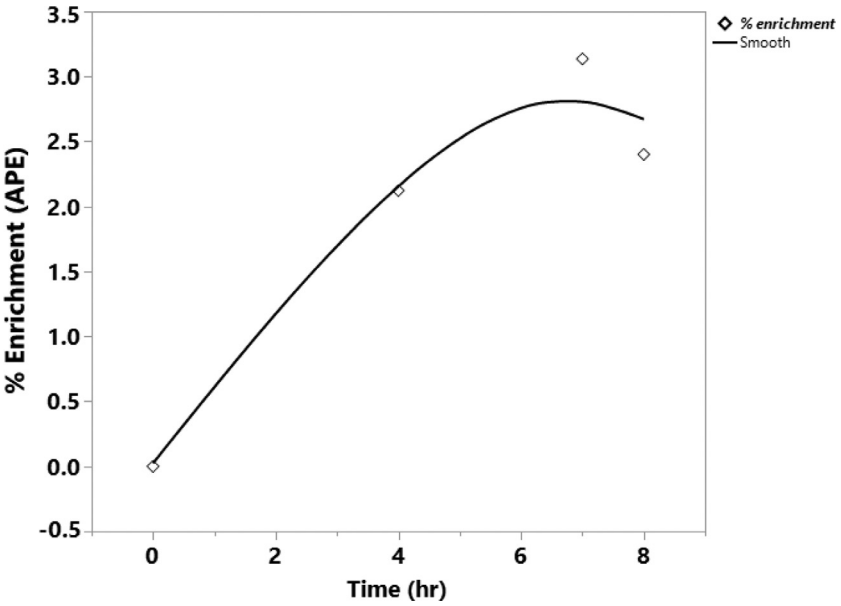

Figure 1. Enrichment curve of deuterium oxide (^2H_2O) in plasma. ^2H_2O was infused intra-peritoneal to broiler as priming dose and then supplemented via drinking water during 8-hr exposure period to reach the target enrichment of ~ 2.5 % atom percent excess (APE) in plasma body water.

expressed as defined by the false discovery rate (FDR) for all three ages analyzed. Furthermore, for understanding and identifying the pathways and physiological processes enriched due to the DE genes, those significant DE genes were subjected to further analysis using the Database for Annotation, Visualization and Integrated Discovery (DAVID) (Version 6.8) and Ingenuity Pathways Analysis (Ingenuity System, Qiagen, 2020).

In-vivo TG Synthesis in Adipogenic Tissue Follow-up study was conducted to understand the *in-vivo* TG synthesis occurring in adipogenic tissue between WB myopathy and non-myopathy groups using a separate set of broiler. The experiment was conducted in a fast-growing commercial meat-type broiler strain at the end of the finisher grow-out period (d49) that were fed diets (Supplementary Table 1) meeting nutrient guidelines as recommended by primary breeder nutrition for the strain (IACUC protocol #19040). Broiler were randomly selected and scored for WB myopathy from the scale of 0−3 (Tijare et al., 2016), then two treatment groups- myopathy (WB score $\geq$ 2) and non-myopathy (WB score $\leq$ 0.5) were created. For each group of non-myopathy and myopathy, $n = 9$ replicate broiler were selected with a total of 20 broiler utilized in the study. Two broiler were utilized for collecting baseline tissue and blood samples from each treatment group.

^2H_2O Tracer Infusion An intraperitoneal injection of $^2H_20$ (99.8 %) (CAS,7789-20-0, Cambridge Isotope Laboratories, Inc., MA, USA) was given to each broiler as a priming dose and supplemented with $^2H_20$ via drinking water to obtain the target of at least 2.5 % of atom percent enrichment (**APE**) of ^2H in plasma water during the experimental $^2H_20$ exposure (Turner et al., 2003; Bederman et al., 2009;) . Blood samples (~ 1 ml) were taken at three different time occasions: 4, 7 and 8-hours post priming dose using the brachial vein and then plasma was separated from the collected blood samples. Tissue samples (liver, fat pad and *P. major* (anterior-cranial)) were collected after completing the 8-hr interval blood collection and euthanizing the broiler with CO_2.

Measurement of ^2H Labelling of Water in Plasma The ^2H-enrichment of water in plasma was determined by procedure reported by Shah et al. (2010). Briefly, 5 ul of plasma sample was taken in 2-ml glass screw-top GC vial and then mixed with 2 ul of 10 N KOH. 5 ul of 99.9% acetone (Millipore Sigma, CAS 650501) was then added and capped immediately. The mixture was allowed to stand for 4 hrs at RT. Gas-chromatographer-mass spectrometer (Agilent Tech, 7890A GC system, 5975C VL MSD, Santa Clara, CA) was utilized for the headspace injection of the sample prepared using the EI and SIM mode with the instrument parameters discussed in Shah et al., (2010). The enrichment of ^2H in plasma water was determined by first creating a standard curve with ^2H concentration generated from the ^2H_2O standard solution following the same procedures as the plasma samples and utilizing the GC-MS. The m/z of the 58 and 59 were determined to understand the ^2H enrichment in plasma water. Figure 1 gives the typical APE enrichment curve post-exposure of ^2H_2O during the experimental period.

TG Isolation from Liver, Muscle, and Fat pads and Measurement of ^2H Enrichment in TG-Glycerol The lab procedures for the TG isolation from tissue samples (liver, muscle (*P. major*), and fat pads) were followed as discussed elsewhere (Pan et al., 1997; Turner et al., 2003; Bederman et al., 2009). Briefly, 50 mg tissue was weighed into a glass, screw-top tube. 200 ul of KOH-ETOH (1M KOH in 70 % Ethanol) was then added to the tube and heated at 80 °C for 3 hours. 50 ul of 6 N HCL was then added to the solution followed by the addition of 300 ul of chloroform. The solution was vortexed for 2 min and centrifuged for 10 m at 12,000 rpm.

The top aqueous and/or glycerol layer was carefully transferred to microcentrifuge tubes and then dried using the liquid N_2. The dried residue was then derivatized using tert−butyldimethylsilyl (tBDMS (Sigma, CAS Number 77377-52-7) before running the samples in GC-MS at EI/SIM mode. The ions were monitored for m/z ratio of 377 (MO), 378 (M1), and 378 (M2) to understand the enrichment of ^2H TG-glycerol in the infused broiler.

Measurement of Fractional Synthesis Rate and Data Analysis The isotopic enrichment of ^2H in glycerol that was derived from the TG-glycerol in infused broiler was measured by first subtracting the mass isotopomer abundances in unlabeled TG-glycerol from the baseline or non-infused broiler. Newly synthesized fraction of TG during the study ^2H_2O exposure was measured by using the precursor-product principle as discussed elsewhere (Turner et al., 2003; Bederman et al., 2009) using the following equation.

$$FSR = M_{1\ glycerol}/A^{\infty}_{1\ glycerol}$$

Where $M_{1glycerol}$ is the mass +1 −labeled species of TG-glycerol in excess of baseline abundance or non-infused tissue, and $A^{\infty}_{1\text{-glycerol}}$ represents the theoretical plateau value or asymptotic value for fully labeled TG-glycerol.

The Fractional Synthesis Rate (FSR) values were obtained for all the sample replicates and corrected for ^2H_2O exposure. The values were then expressed in %/hr. The obtained FSR values were then subjected to data analysis using JMP Pro 14 (SAS Institute, Inc., Cary, NC). Significant means for FSR values were separated using the Tukey HSD test at P-value < 0.05.

RESULTS

RNA-Seq Analysis

The DE genes are expressed in log2 fold change (FC) >1 or <-1, where positive values represent the upregulated genes, and the negative values represent the downregulated genes. Furthermore, the DE genes along with the FC values were subjected to Ingenuity Pathway Analysis to understand the possible biological and molecular pathways involved in myopathy affected broiler in relation to non-myopathy broiler. The IPA database for pathways analysis or molecules involved in the biological system based on the DE gene has been developed based on the ortholog or homologous genes derived mainly from humans, mice and rats. Therefore, genes that were first identified and confirmed for *Gallus gallus* species (using DAVID) for subjecting to IPA analysis. The DE genes (at $P < 0.05$) were then reported that have possible etiopathological significances for WB myopathy condition in broiler.

D 21 Expression Analysis

The differentially expressed genes for myopathy broiler (at FDR ≤ 0.05) were reported based on the etiological significance (Figure 2). The upregulated genes were BTG family, member 2 (BTG2), OTU domain containing 1 (OTUD1), and zinc finger protein 236 (ZNF236).

Top bio-functions affected as predicted by IPA expression analyses were related to cell cycle and cellular development (Table 1). Top physiological systems that were affected were mainly related to skeletal and muscular development, and connective tissue development. There were four upregulated molecules as predicted by the IPA (Table 2).

D 42 Expression Analysis

The 12 DE genes that were of etiological significance for myopathy broiler (at FDR < 0.01) are reported (Figure 3). The downregulated genes for myopathy broiler were related to carbohydrate transport and metabolism (PYGB and MGAM), cell membrane integrity (ACHE, DPP4, APCDD1, LOC423849, EHA10, MSANTD4, CSMD3 and ADAM20), and calcium signaling pathway (LOC423134). The upregulated genes were related to muscle growth (IGF1), regulation of blood pressure and vasodilation (UTS2R), and ubiquitin (SACS).

Top bio-functions (Table 1) affected as predicted by IPA expression analyses were related to carbohydrate metabolism and cell cycle and cellular functions and maintenance. Top physiological systems that were affected were mainly related to skeletal and muscular development, and cardiovascular system development and function. There were 8 upregulated and nine downregulated molecules as predicted by IPA (Table 2).

D 56 Expression Analysis

The 14 DE genes that were of etiological significance for myopathy broiler (at FDR < 0.05) are reported (Figure 4). The upregulated genes were related to responses to hypoxia and/or calcium signaling (CXCR4 and HMOX1), membrane integrity (ADORA1, RASL11A, RETSAT, and SSTR2), carbohydrate metabolism (ALDOB and GPD1L2), fatty acid binding (FABP4, LOC425531, and RBP7), and apoptotic (CIDEC). The downregulated genes expressed were related to tight junction or extracellular region (MYH1D and PENK).

Top bio-functions affected as predicted by IPA expression analyses were related to lipid metabolism and molecular transport (Table 1). Top physiological systems that were affected were mainly related to skeletal and muscular development, and cardiovascular system development and function. There were 10 upregulated molecules and three downregulated molecules as predicated by IPA and their associated functions are presented (Table 2).

In-vivo TG synthesis in Adipogenic Tissue

Liver The *in-vivo* TG FSR observed in liver for non-myopathy broiler was 0.197 %/hr which was higher compared to myopathy broiler which was occurring at

Table 1. Top two bio-functions affected in myopathy broiler at three different grow-out ages as predicted by IPA expression analysis*.

Day	Molecular and Cellular functions	Physiological System Development and Functions
21	Cell cycle (2); Cellular development (2)	Skeletal and muscular system (2); Connective tissue development and function (2)
42	Carbohydrate metabolism (31); Cellular functions and maintenance (39)	Skeletal and muscular system (34); Cardiovascular system development and function t (38)
56	Lipid metabolism (7); Molecular transport (10);	Skeletal and muscular system (7); Cardiovascular system development and function (6)

*The number in the parenthesis represents number of molecules affected with the associated functions.

Table 2. Top analysis-ready molecules expression log ratio for differentially expressed significant genes for myopathy broiler at three different ages of broiler grow-out period.

Molecules	Gene name	Major molecular functions/regulations	Expression Log ratio
		Day 21 expression	
ZNF236	Zinc finger protein 236	Transcription regulators; Hypertension effects	3.82
FOS	Fos proto-oncogene	Apoptosis; Differentiation	1.51
OTUD1	OTU deubiquitinase 1	Ubiquitin-specific protease	1.418
BTG2	BTG anti-proliferation factor 2	Apoptosis; Differentiation	1.3
		Day 42 expression	
IGF1	Insulin like growth factor 1	Skeletal system development; Blood vessel remodeling; Skeletal system development	4.723
UTS2R	Urotensin 2 receptor	Elevation in, proliferation, growth, expression in	4.62
SACS	Sacsin molecular chaperone	Protein folding	4.529
NOVA1	NOVA alternative splicing regulator 1	Apoptosis, splicing by, invasion by, migration, proliferation	4.142
AKAP6	A-kinase anchoring protein 6	cAMP-mediated signaling; Positive regulation of release of Sequestered calcium ion into cytosol	3.826
BMP5	Bone morphogenetic protein 5	Apoptosis; Differentiation	3.043
AGAP3	ArfGAP with GTPase domain	Proteasomal ubiquitin-dependent protein catabolic process	2.894
CDK2AP1	Cyclin-dependent kinase 2 associated protein 1	Apoptosis, growth, function, cell viability	2.775
LOC100910977	Disintegrin and metalloproteinase domain-containing protein 25-like	Metalloendopeptidase activity; Proteolysis	-5.866
P2RX3	Purinergic receptor P2×3	Action potential	-4.822
FFAR2	Free fatty acid receptor 2	Cell surface pattern recognition receptor signaling pathway; Cellular response to fatty acid; Fat cell differentiation; Glucose homeostasis	-4.788
APOB	apolipoprotein B	Artery morphogenesis; Lipid metabolic process; Lipid transport; Lipoprotein biosynthetic process	-4.739
SPI1	Spi-1 proto-oncogene	Vasculature development, abnormal morphology, proliferation, apoptosis	-4.371
HSD11B2	Hydroxysteroid 11-beta dehydrogenase 2	Response to hypoxia; Glucocorticoid biosynthetic process	-4.364
RHAG	Rh associated glycoprotein	Cellular ion homeostasis	-3.928
TAL1	Erythroid differentiation factor	Angiogenesis	-3.886
		Day 56 expression	
RBP7	Retinol binding protein 7	Lipid binding	3.913
CIDEC	Cell death inducing DFFA like effector c	Apoptotic process; execution phase of apoptosis; Lipid particle organization; Regulation of apoptotic process	3.576
IGFALS	Insulin like growth factor binding protein acid labile subunit	Aging; Cresponse to interleukin 1	3.296
SSRT2	Somatostatin receptor 2	Negative regulation of cell proliferation	3.234
FABP4	Fatty acid binding protein 4	Positive regulation of fat cell proliferation	3.169
ALDOB	Aldolase, fructose-bisphosphate B	Gluconeogenesis I; Glycolysis I;	2.831
RASL11A	RAS like family 11 member A	Positive regulation of transcription from RNA polymerase I promoter	2.822
CXCR4	C-X-C motif chemokine receptor 4	Apoptotic process; Response to hypoxia	2.498
ADORA1	Adenosine A1 receptor	Integral to membrane; Integral to plasma membrane; Response to hypoxia	2.288
RETST	Retinol saturase	Oxidation-reduction process	2.239
PENK	Proenkephalin	Plasma membrane	-1.8
MYH2	Myosin heavy chain 2	Plasma membrane repair; Calcium Signaling	-1.331
KCNJ11	Potassium inwardly rectifying channel subfamily J member 11	Negative regulation of insulin secretion	-1.0401

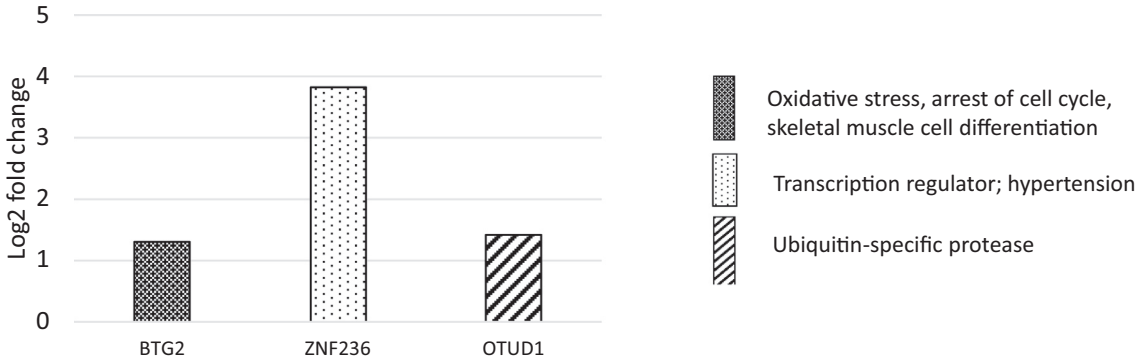

Figure 2. Differentially expressed genes (log2 fold change) at d 21 for myopathy broiler in relation to non-myopathy broiler*.*BTG family, member 2(BTG2); zinc finger protein 236(ZNF236); OTU domain containing 1(OTUD1).

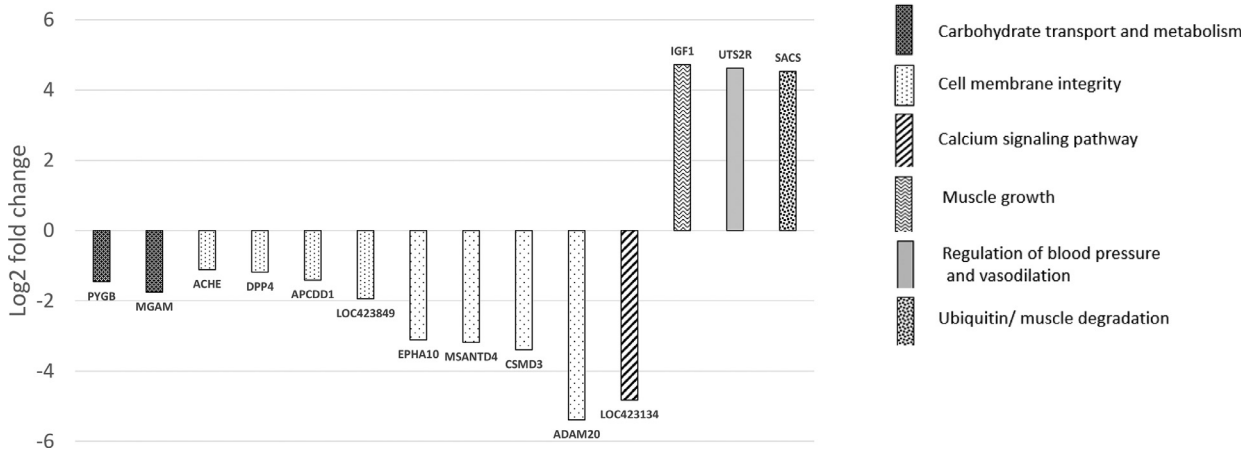

Figure 3. Differentially expressed genes (log2 fold change) at d 42 for myopathy broilers in relation to non-myopathy broiler*.*phosphorylase, glycogen; brain(PYGB); maltase-glucoamylase (alpha-glucosidase)(MGAM); acetylcholinesterase (Yt blood group)(ACHE); dipeptidyl-peptidase 4(DPP4); adenomatosis polyposis coli down-regulated 1(APCDD1); prominin 1-like(LOC423849); EPH receptor A10(EPHA10); Myb/SANT DNA binding domain containing 4 with coiled-coils(MSANTD4); CUB and Sushi multiple domains 3(CSMD3); ADAM metallopeptidase domain 20(ADAM20); Insulin growth facto 1(IGF1); proteoglycan 2, bone marrow-like(LOC423134); urotensin 2 receptor(UTS2R); sacsin molecular chaperone(SACS).

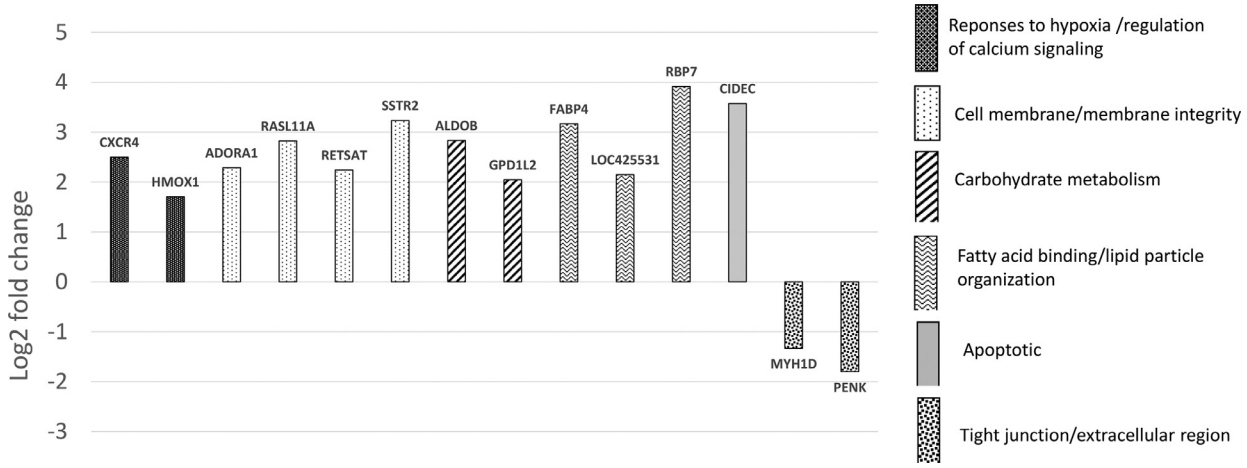

Figure 4. Differentially expressed genes (log2 fold change) at d 56 for myopathy broiler in relation to non-myopathy broiler*.*C-X-C motif chemokine receptor 4(CXCR4); adenosine A1 receptor(ADORA1); RAS-like, family 11, member A(RASL11A); aldolase B, fructose-bisphosphate (ALDOB); cell death inducing DFFA like effector c(CIDEC); fatty acid binding protein 4, adipocyte(FABP4); glycerol-3-phosphate dehydrogenase 1-like 2(GPD1L2); heme oxygenase 1(HMOX1); myosin, heavy chain 1D, skeletal muscle (similar to human myosin, heavy chain 1, skeletal muscle, adult)(MYH1D); proenkephalin(PENK); ras-related protein Rab-18-B-like(LOC425531);retinol binding protein 7, cellular(RBP7); retinol saturase (all-trans-retinol 13,14-reductase)(RETSAT); somatostatin receptor 2(SSTR2).

0.123 %/hr ($P = 0.0479$; Figure 5. i). All the replicate broiler for both treatment groups in the study showed the detectable synthesis rates with the given tracer exposure time (8-hour period) in the study.

Pectoralis Major Muscle The TG FSR values observed in *P. major* for WB myopathy broiler was 0.015%/hr compared to 0.002%/hr for non-myopathy broiler ($P = 0.0736$) (Figure 5. ii). There was one

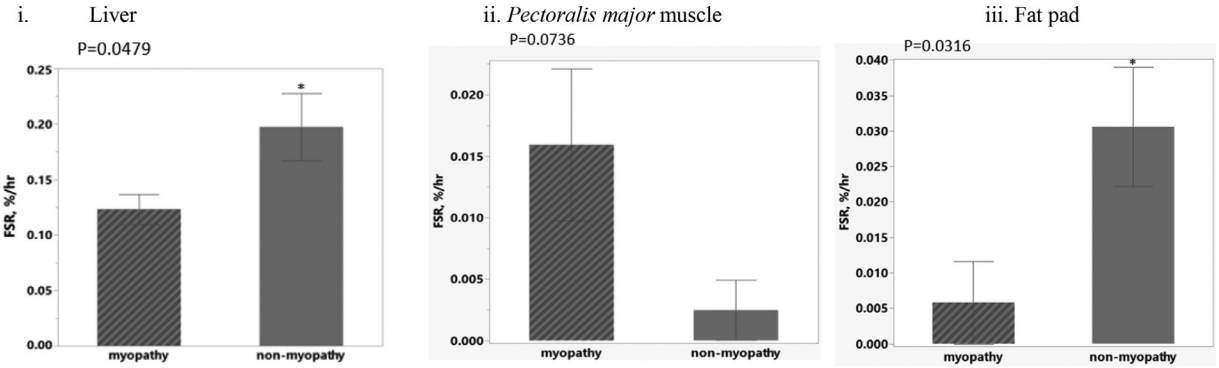

*n=9 replicates/treatment group for liver, *Pectoralis major* and fat pad tissues

Figure 5. *In-vivo* triglyceride fractional synthesis rates in adipogenic tissues at d 49 for myopathy broilers and non-myopathy broiler*

replicate broiler with myopathy group that had non-detectable TG synthesis (~ 0 %/hr) compared to six replicate broilers in non-myopathy group.

Abdominal Fat Pads The TG FSR values observed in abdominal fat pads for WB myopathy broiler was 0.005%/hr compared to 0.030 %/hr for non-myopathy broiler ($P = 0.0316$; Figure 5. iii). There were seven replicate broilers with myopathy group that had non-detectable TG synthesis (~ 0 %/hr) compared to three replicate broiler in non-myopathy group.

DISCUSSION

Involvement of Physiological Systems

Metabolic disorders are becoming more evident in high yielding meat broiler lines due to the adverse response of these broiler strains to selection pressure for growth rate and meat yield. Of many metabolic and physiological perturbations that high-yielding broiler may encounter, it was predicted that skeletal muscle related metabolic disorder could remain as a major challenge for poultry industry (Leeson, 2007). The industry is witnessing the myopathy condition, called WB myopathy, which is of idiopathic origin. The transcriptomic changes for myopathy broiler from the present study were related to skeletal and muscular system, connective tissue development, and cardiovascular system (Table 1). The cardiovascular system related change in gene expression in myopathy broiler occurred at later ages (d 42 and d 56) in broiler grow-out period (Table 1). The IPA analysis of the present study on the major physiological phenomena at the early age (d 21) of the WB affected *P. major* muscle showed the involvement of connective tissue development which was not observed at the later ages (d 42 and d 56). Maharjan et al. (2020a,c)) reported a higher FSR (in %/hr) of collagenous connective tissue occurring for myopathy broiler at an earlier age (d 21) compared to non-myopathy broiler. The research group outlined the *in-vivo* FSR rates for collagen connective tissue in myopathy broiler were almost non-detectable on %/hr basis at d 42 and d 56. The reduced FSR values of collagen at finishing phase of broiler grow-out period could be an adaptive physiological feedback mechanism of the broiler against excessive synthesis and deposition of extracellular collagen beyond a supportive role (Kjær, 2004; Waterlow et al., 1978). Musculoskeletal physiological involvement could be more related to changes in the *in-vivo* turnover (synthesis and degradation rates) of mixed muscle, which are discussed in detail below.

Initial studies on transcriptomic and metabolomic findings on myopathy broiler were based on one age or single point sampling; however, the findings reported in those studies were similar to the current study revealing the possible involvement of the cardiovascular symptoms such as localized hypoxia and oxidative stress (Mutryn et al, 2015; Abasht et al., 2016; Maharjan et al. 2019). Similarly, past metabolomic findings showed the elevated expression of metabolites such as homocysteine, trimethylamine N-oxide, tyramine, N-glutamic acid, carnitine and acetyl carnitine in plasma which suggested the possible involvement of cardiovascular disease (Wierzbicki, 2007; Maharjan et al., 2019). Another transcriptomic study performed in myopathy broiler using RNA-Seq also showed molecular perturbations involving vasculature (Papah et al., 2018). Similarly, the genes related to hypoxia were upregulated in WB affected muscle fibers (Malila et al., 2019) which were also evident in d 42 (UTS2R) and d 56 (CXCR4 and HMOX 1) findings of the present study. The UTS2R is a potent known vasoconstrictor (Clozel et al., 2004a) that could bring ischemia due to hypoxic condition. The probable ongoing hypoxic condition with WB myopathy would be further confirmed by the microscopical morphometry that showed the reduced vessel density and compromised blood supply in affected tissue (Sihvo et al., 2018; Pampouille et al., 2019). In response to hypoxia, there is an activation of CXCR4 and HMOX1 genes to enhance the oxygen homeostasis in cells (Schioppa et al., 2004; Ishikawa et al., 2009).

Elevated Expression of Muscle Degradation and Synthesis Rates

Studies on metabolic and physiological findings have showed the higher *in-vivo* muscle degradation rates occurred in myopathy broiler compared to non-myopathy (Abasht et al., 2016; Maharjan et al., 2019; Maharjan et al., 2020c). The higher degradation of mixed muscle proteins occurred in the *P. major* could be further complemented by significant higher expression of genes related to oxidative stress (BTG2, ZNF236, CXCR4, HMOX1) and hypertensive effects (ZNF236 and UTS2R) in the WB affected muscle as found in the present study. The hypertensive and atherogenic effects (of metabolites) could also compromise the blood supply in the affected muscle tissue leading to atrophy and degradation, which could be one pathophysiological condition occurring in myopathy broiler. Furthermore, there were downregulation of several genes related to cell membrane integrity (ACHE, DPP4, APCDD1, LOC423849, EPHA10, CSMD3, and ADAM 20) and upregulation of the gene related to muscle degradation (SACS) (Figure 3). Deubiquitanases have roles in removing ubiquitin from the target protein or ubiquitin chain, and ubiquitin precursor polypeptides to create ubiquitin homeostasis in cells (Komander et al., 2009). Genes related to deubiquitinases such as ubiquitin-specific proteases are expressed higher with myopathy broiler at d 21 and d 42 (OTUD1 and SACS, respectively) that play role in steady state availability of monoubiquitin and regulation of substrate degradation at the proteasome (Reyes-Turcu et al., 2009). Earlier studies also reported the higher mixed muscle degradation rates in myopathy broiler compared to non-myopathy (Maharjan et al., 2020c), the potential phenomenon responsible for leaving the space for connective tissue growth and lipid deposition when WB myopathy is concurrently occurring with white striping of muscle (Kuttappan et al., 2016; Vignale et al., 2017).

Another factor that could enhance the muscle degeneration and degradation could be arising from the energy status of cells. The expression of genes such as PYGB and MGAM which were related to carbohydrate transport and metabolism were down-regulated at d 42 which indicated that the WB affected myofibers could be undergoing nutrient and/or energy-deficient mode of the cell. The proteomic and metabolic studies revealed a reduced expression of carbohydrate metabolism and glycogen levels in affected tissue (Abasht et al., 2016; Kuttappan et al., 2017). An important revelation of this study was related to d 56 differential gene expression results that showed WB myopathy broiler tended to respond to the nutrient-deficient mode of cells by upregulating the genes that enhanced the carbohydrate metabolism (ALDOB, GPD1L2), cell membrane integrity (ADORA1, RASL11A, RETSTAT, SSTR2), response to hypoxia (CXCR4, HOMX1), and fatty acid metabolism (FABP4, lOC425531, and RBP) (Figure 4). The response to the nutrient-deficient mode of cells by the increased expression levels of genes related to carbohydrate metabolism, cell membrane integrity, response to hypoxia, and fatty acid metabolism could be potential ongoing physiological feedback mechanism of myopathy affected broiler. ALDOB is involved in glycolytic-gluconeogenic pathway that catalyzes the fructose-1-phosphate into glyceraldehyde and dihydroacetone phosaphate (DHAP). Glyceraldehyde is phosphorylated to form glycerol-3 phosphate (G3P) that can generate glucose pyruvate in glycolytic-gluconeogenic pathway (Feinman and Fine, 2013). GPD1L2 have roles both in reversible conversion of DHAP to G3P and have roles in increased lipid biosynthesis via increased glycerol production (Ou et al., 2006). FABP have roles in FA uptake and transport and affect the intracellular lipid homeostasis ultimately affecting the energy homeostasis (Storch and McDermott, 2009).

A proteomic analysis of network and biological pathways indicates eukaryotic initiation factor-2 (eIF-2), mechanistic target of rapamycin (mTOR), eIF4, and p70S6K are upregulated in *P. major* of myopathy broiler (Kuttappan et al., 2017). The up-regulation of these pathways indicated an ongoing higher muscle synthesis rates and muscle hypertrophy. The broiler needed the increased muscle degradation balanced with increased synthesis rates. The findings of the present study also showed the genes related to transcription factors, muscle cell differentiation (ZNF234, BTG2), and muscle growth (IGF1) were upregulated at early grow-out period (d 21) and again in later finishing period (d 42). The higher expression of muscle specific transcription factors and resultant muscle differentiation and growth could be resulting from the muscle regeneration occurring in myopathy broiler in response to higher muscle degradation and damage (Velleman and Clark, 2015; Maharjan et al., 2020c).

Altered in-vivo *Triglyceride Synthesis in Adipogenic Tissues*

The ^{2}H isotopic label using $^{2}H_2O$ was utilized to understand the *in-vivo* TG kinetics. The $^{2}H_2O$ technique as a metabolic tracer is relatively non-invasive and has not been reported in broiler species to study nutrient turnover which could open the avenues for further research to understand lipid kinetics using this methodology. The acylglycerides made from intracellular α-glycerol phosphate during $^{2}H_2O$ exposure contain the labelled hydrogen atoms integrated from tissue body water. The hydrogen in C-H of the glycerol moiety in α-glycerol phosphate forming acylglycerides will either be of single mass unit or double mass unit, thus allowing to help measure the newly synthesized versus pre-existing acylglycerides during the $^{2}H_2O$ label exposure. Hydrogen exchange does not occur between water and C-H bonds after α- glycerol phosphate is bound to acyl groups (Turner et al., 2003). Acylglyceride with ^{2}H in its α-glycerol moiety had to be assembled from α-glycerol phosphate.

The transcriptomic findings of *P. major* muscle from the current study found the major genes affected on molecular and cellular functions were related to molecular transport and maintenance including lipid metabolism for myopathy broiler (Table 1 and Table 2). Understanding the i*n-vivo* TG synthesis may provide an insight that could be associated with lipid disorders with myopathy broiler**.** The increased lipidosis was observed in histological or compositional analysis in other studies (Kuttappan et al., 2013; Mudalal et al., 2014; Petracci et al., 2015; Papah et al., 2017) in WB affected muscle, which could be arising from the event of vascular complexity in meat broiler. This was evidenced by higher TG FSR values with myopathy group and with higher number of replicate broiler at detectable range of TG synthesis in *P. major* muscle found in this study (Figure 5. ii)**.**

All metabolic processes of uptake, synthesis, storage, secretion, and catabolism of fatty acids (**FAs**) and TGs can take place in liver. Under normal condition, liver stores only a small amount of FAs in the form of TG, and most TG synthesized are secreted into bloodstream as TG-enriched very low-density lipoprotein (VLDL-TG) (Alves-Bezerra and Cohen, 2011). TG molecules are the principal means by which liver export FAs that are delivered to muscle for oxidation and fat tissues for storage, depending on the nutritional and physiological states of animal. The WB affected myofibers have reduced carbohydrate metabolism (reduced expression of glycolysis and gluconeogenesis) producing the energy deficient state of cells (Kuttappan et al., 2017). This potentially could lead to increased demand and utilization of FAs in the WB affected muscle to fulfill energy need of cells, which could result in reduced turnover or secretion of FAs into blood circulation. The sub-optimal availability of FAs in the circulation could lead to its reduced re-esterification for TG synthesis in liver compared to non-myopathy broiler (Figure 5. i). Furthermore, there could be possibility of another physiological cascade that the majority of TG synthesized in liver with WB myopathy affected broiler could be delivered to muscle (*P. major*) (than to fat pad storage) to fulfil the increased need of energy (via TG lipolysis and FA oxidation) of cells. Therefore, there was reduced TG FSR and reduced number of myopathy broiler that had detectable TG synthesis in fat pads compared to non-myopathy broiler (Figure 5. iii). Since more TG directed to muscle in WB affected muscle are regulated to release FAs, there could be increased concurrent re-esterification of FA to glycerol to form TGs that could have resulted in greater TG FSR values with myopathy group with more number of replicate broiler having detectable TG synthesis (in %/hr basis) compared to non-myopathy group (Figure 5.ii). This also explains more lipidosis occurring *in P. major* with the myopathy group compared to non-myopathy group. The upregulation of transcription factors or mTOR that was mentioned earlier in the discussion with myopathy affected muscle may also regulate lipid synthesis by increasing the expression of peroxisome proliferator-activated receptor γ (PPARγ) which could positively impact the adipogenesis (Le Bacquer et al., 2007; Zhang et al, 2009). The overall findings also open up the question that if more lipoprotein lipase (LPL) are expressed in the lumen surface of muscle (than in adipose tissue) capillaries aiding in more VLDL release of TG in the muscle of myopathy broiler as compared to non-myopathy broiler. Furthermore, there is clearly a co-ordination that was occurring between liver, muscle, and fat pads for optimal mobilization of TG in accordance with cellular physiological state of these tissues to fulfill the increased need of FAs in muscle cells of myopathy broiler. Wagenmakers et al. (2006) earlier discussed the coordinated use of TG and its mobilization (or hydrolysis) to release FAs in a regulated way between liver, muscle, and adipose tissue in mammals.

In conclusion, the timeline transcriptomic analysis of *P. major* of WB myopathy broiler exhibited genes associated to hypoxia and oxidative stress, carbohydrate metabolism, muscle growth, calcium signaling, and cell membrane integrity were expressed differently (towards the adaptive physiological feedback responses to adverse cellular states) at d 56 than at earlier grow-out period at d 21 and d 42 (Figures 2-4; Table 1-2). The top physiological systems that were affected in WB myopathy broiler were connective tissue, musculo-skeletal, and cardiovascular systems. These alterations in physiological processes possibly produced histological and pathophysiological consequences in muscle tissue such as excessive synthesis and deposition of extracellular matrix (possibly collagen), localized hypoxia, and an energy deficient state of myofibers. The altered physiological processes synchronously resulted in massive degradation and synthesis of muscle fiber along with altered TG kinetics in adipogenic tissues. The approach of adaptive feedback responses as observed with age (at d 56) to metabolic shift of meat broiler lines against hypoxia and oxidative stress or the signs of inflammatory, regeneration, fibrosis, and slower *in-vivo* synthesis rates of collagenous extracellular matrix in *P. major* have been previously conceptualized (Williams and Athrey, 2018; Pampouille et al., 2019; Maharjan et al., 2020b).

ACKNOWLEDGEMENTS

The authors acknowledge Cobb Vantress, Inc. for their generous support by funding this project. Authors would also like to thank Prahlad K. Rao and Michelle Puchowicz from the Department of Pediatrics, The University of Tennessee Health Science Center for answering queries related to the tracer kinetics on lipid work.

DISCLOSURES

The authors declare no conflicts of interest.

SUPPLEMENTARY MATERIALS

Supplementary material associated with this article can be found in the online version at https://doi.org/10.1016/j.psj.2021.101092.

REFERENCES

Abasht, B., M. F. Mutryn, R. D. Michalek, and W. R. Lee. 2016. Oxidative stress and metabolic perturbations in wooden breast disorder in chickens. PLoS One 11 e0153750.

Alves-Bezerra, M., and D. E. Cohen. 2011. Triglyceride metabolism in the liver. Compr. Physiol. 8:1–22.

Bailey, R. A., K. A. Watson, S. F. Bilgili, and S. Avendano. 2015. The genetic basis of pectoralis major myopathies in modern broiler chicken lines. Poult. Sci. 94:2870–2879.

Bederman, I. R., S. Foy, V. Chandramouli, J. C. Alexander, and S. F. Previs. 2009. Triglyceride synthesis in epididymal adipose tissue contribution of glucose and non-glucose carbon sources. J. Biol. Chem. 284:6101–6108.

Calvi, E. N., D. C. Nahas, F. X. Barbosa, M. V. Calil, J. A. Ihara, S. S. M. Silva, M. D. S. Franco, M. F. D. and L. M. Ferreira. 2012. An experimental model for the study of collagen fibers in skeletal muscle. Acta Cirurgica Bras. 27:681−68

Clozel, M., C. Binkert, M. Birker-Robaczewska, C. Boukhadra, S. Ding, W. Fischli, P. Hess, B. Mathys, K. Morrison, and C. Müller. 2004. Pharmacology of the urotensin-II receptor antagonist palosuran (ACT-058362; 1-[2-(4-benzyl-4-hydroxy-piperidin-1-yl)-ethyl]-3-(2-methyl-quinolin-4-yl)-urea sulfate salt): first demonstration of a pathophysiological role of the urotensin system. J. Pharmacol. Exp. Ther. 311:204–212.

Feinman, R. D., and E. J. Fine. 2013. Fructose in perspective. Nutr. Metab. 10:1–12.

Ishikawa, T., K. Nakashiro, S. K. Klosek, H. Goda, S. Hara, D. Uchida, and H. Hamakawa. 2009. Hypoxia enhances CXCR4 expression by activating HIF-1 in oral squamous cell carcinoma. Oncol. Rep. 21:707–712.

Kjær, M. 2004. Role of extracellular matrix in adaptation of tendon and skeletal muscle to mechanical loading. Physiol. Rev. 84:649–698.

Komander, D., M. J. Clague, and S. Urbé. 2009. Breaking the chains: structure and function of the deubiquitinases. Nat. Rev. Mol. Cell Biol. 10:550–563.

Kuttappan, V. A., W. Bottje, R. Ramnathan, S. D. Hartson, C. N. Coon, B. Kong, C. M. Owens, M. Vazquez-Añon, and B. M. Hargis. 2017. Proteomic analysis reveals changes in carbohydrate and protein metabolism associated with broiler breast myopathy. Poult. Sci. 96:2992–2999.

Kuttappan, V. A., B. M. Hargis, and C. M. Owens. 2016. White striping and woody breast myopathies in the modern poultry industry: a review. Poult. Sci. 95:2724–2733.

Kuttappan, V. A., H. L. Shivaprasad, D. P. Shaw, B. A. Valentine, B. M. Hargis, F. D. Clark, S. R. McKee, and C. M. Owens. 2013. Pathological changes associated with white striping in broiler breast muscles. Poult. Sci. 92:331–338.

Le Bacquer, O., E. Petroulakis, S. Paglialunga, F. Poulin, D. Richard, K. Cianflone, and N. Sonenberg. 2007. Elevated sensitivity to diet-induced obesity and insulin resistance in mice lacking 4E-BP1 and 4E-BP2. J. Clin. Invest. 117:387–396.

Leeson, S. 2007. Metabolic challenges: past, present, and future. J. Appl. Poult. Res. 16:121–125.

Liao, Y., G. K. Smyth, and W. Shi. 2019. The R package Rsubread is easier, faster, cheaper and better for alignment and quantification of RNA sequencing reads. Nucleic Acids Res. 47:e47.

Maharjan, P., K. Hilton, J. Weil, N. Suesuttajit, A. Beitia, C. Owens, and C. Coon. 2019. Characterizing Woody Breast Myopathy in a Meat Broiler Line by Heat Production, Microbiota, and Plasma Metabolites. Front. Vet Sci. 6:497.

Maharjan, P., G. Mullenix, K. Hilton, A. Beitia, J. Weil, N. Suesuttajit, D. Martinez, C. Umberson, J. England, and J. Caldas. 2020a. Effects of dietary amino acid levels and ambient temperature on mixed muscle protein turnover in Pectoralis major during finisher feeding period in two broiler lines. J. Anim. Physiol. Anim. Nutr. 104:1351–1364.

Maharjan, P., C. M. Owens, and C. Coon. 2020b. In-vivo Intramuscular Collagen Synthesis, Muscle Fiber Growth and Histomorphology of Pectoralis major of a Fast-Growing Broiler Strain Gallus gallus domesticus. Front. Vet. Sci. 6:470.

Maharjan, P., J. Weil, A. Beitia, N. Suesuttajit, K. Hilton, J. Caldas, C. Umberson, D. Martinez, C. M. Owens, and C. Coon. 2020c. In vivo collagen and mixed muscle protein turnover in 2 meat-type broiler strains in relation to woody breast myopathy. Poult. Sci. 99:5055–5064.

Malila, Y., K. Thanatsang, S. Arayamethakorn, T. Uengwetwanit, Y. Srimarut, M. Petracci, G. M. Strasburg, W. Rungrassamee, and W. Visessanguan. 2019. Absolute expressions of hypoxia-inducible factor-1 alpha (HIF1A) transcript and the associated genes in chicken skeletal muscle with white striping and wooden breast myopathies. PLoS One 14: e0220904.

Mudalal, S., E. Babini, C. Cavani, and M. Petracci. 2014. Quantity and functionality of protein fractions in chicken breast fillets affected by white striping. Poult. Sci. 93:2108–2116.

Mutryn, M. F., E. M. Brannick, W. Fu, W. R. Lee, and B. Abasht. 2015. Characterization of a novel chicken muscle disorder through differential gene expression and pathway analysis using RNA-sequencing. BMC Genomics 16:399.

Ou, X., C. Ji, X. Han, X. Zhao, X. Li, Y. Mao, L. Wong, M. Bartlam, and Z. Rao. 2006. Crystal structures of human glycerol 3-phosphate dehydrogenase 1 (GPD1). J. Mol. Biol. 357:858–869.

Pampouille, E., C. Hennequet-Antier, C. Praud, A. Juanchich, A. Brionne, E. Godet, T. Bordeau, F. Fagnoul, E. Le Bihan-Duval, and C. Berri. 2019. Differential expression and co-expression gene network analyses reveal molecular mechanisms and candidate biomarkers involved in breast muscle myopathies in chicken. Sci. Rep. 9:1–17.

Pan, D. A., S. Lillioja, A. D. Kriketos, M. R. Milner, L. A. Baur, C. Bogardus, A. B. Jenkins, and L. H. Storlien. 1997. Skeletal muscle triglyceride levels are inversely related to insulin action. Diabetes 46:983–988.

Papah, M. B., and B. Abasht. 2019. Dysregulation of lipid metabolism and appearance of slow myofiber-specific isoforms accompany the development of Wooden Breast myopathy in modern broiler chickens. Sci. Rep. 9:1–12.

Papah, M. B., E. M. Brannick, C. J. Schmidt, and B. Abasht. 2017. Evidence and role of phlebitis and lipid infiltration in the onset and pathogenesis of Wooden Breast Disease in modern broiler chickens. Avian Pathol. 46:623–643.

Papah, M. B., E. M. Brannick, C. J. Schmidt, and B. Abasht. 2018. Gene expression profiling of the early pathogenesis of wooden breast disease in commercial broiler chickens using RNA-sequencing. PLoS One 13:e0207346.

Petracci, M., S. Mudalal, F. Soglia, and C. Cavani. 2015. Meat quality in fast-growing broiler chickens. Worlds Poult. Sci. J. 71:363–374.

Reyes-Turcu, F. E., K. H. Ventii, and K. D. Wilkinson. 2009. Regulation and cellular roles of ubiquitin-specific deubiquitinating enzymes. Annu. Rev. Biochem. 78:363–397.

Schioppa, T., B. Uranchimeg, A. Saccani, and S. K. Biswas. 2004. Regulation of the chemokine receptor CXCR4 by hypoxia. Minerva Biotecnologica 16:8.

Shah, V., K. Herath, S. F. Previs, B. K. Hubbard, and T. P. Roddy. 2010. Headspace analyses of acetone: a rapid method for measuring the 2H-labeling of water. Anal. Biochem. 404:235–237.

Sihvo, H., N. Airas, J. Lindén, and E. Puolanne. 2018. Pectoral vessel density and early ultrastructural changes in broiler chicken wooden breast myopathy. J. Comp. Pathol. 161:1–10.

Sihvo, H., K. Immonen, and E. Puolanne. 2014. Myodegeneration with fibrosis and regeneration in the pectoralis major muscle of broiler. Vet. Pathol. 51:619–623.

Soglia, F., M. Mazzoni, and M. Petracci. 2019. Spotlight on avian pathology: Current growth-related breast meat abnormalities in broiler. Avian Pathol. 48:1–3.

Storch, J., and L. McDermott. 2009. Structural and functional analysis of fatty acid-binding proteins. J. Lipid Res. 50:S126–S131.

Team, R. C. 2019. R version 3.5. 3: A Language and Environment for Statistical Computing. R Foundation for Statistical Computing, Vienna, Austria. Accessed May 2021. https://www.R-project.org.

Tijare, V. V., F. L. Yang, V. A. Kuttappan, C. Z. Alvarado, C. N. Coon, and C. M. Owens. 2016. Meat quality of broiler breast fillets with white striping and woody breast muscle myopathies. Poult. Sci. 95:2167–2173.

Turner, S. M., E. J. Murphy, R. A. Neese, F. Antelo, T. Thomas, A. Agarwal, C. Go, and M. K. Hellerstein. 2003. Measurement of TG synthesis and turnover in vivo by 2H2O incorporation into the glycerol moiety and application of MIDA. Am. J. Physiol. Endocrinol. Metab. 285:E790–E803.

Velleman, S. G., and D. L. Clark. 2015. Histopathologic and myogenic gene expression changes associated with wooden breast in broiler breast muscles. Avian Dis. 59:410–418.

Vignale, K., J. V. Caldas, J. A. England, N. Boonsinchai, A. Magnuson, E. D. Pollock, S. Dridi, C. M. Owens, and C. N. Coon. 2017. Effect of white striping myopathy on breast muscle (Pectoralis major) protein turnover and gene expression in broiler. Poult. Sci. 96:886–893.

Wagenmakers, A. J., K. N. Frayn, P. Arner, and H. Yki-Järvinen. 2006. Fatty acid metabolism in adipose tissue, muscle and liver in health and disease. Essays Biochem. 42:89–103.

Waterlow, J. C., P. J. Garlick, and D. J. Mill Ward. 1978. Protein Turnover in Mammalian Tissues and in the Whole Body. Elsevier/North-Holland Biomedical Press, 335 Jan van Galenstraat, PO Box 211, 1000 AE Amsterdam, The Netherlands.

Wierzbicki, A. S. 2007. Homocysteine and cardiovascular disease: a review of the evidence. Diabetes Vasc Dis Res. 4:143–149.

Williams, T. J., and G. Athrey. 2018. Insights into the molecular basis of wooden breast based on comparative analysis of fast-and slow-growth broiler.

Wold, J. P., E. Veiseth-Kent, V. Høst, and A. Løvland. 2017. Rapid on-line detection and grading of wooden breast myopathy in chicken fillets by near-infrared spectroscopy. PLoS One 12 e0173384.

Zhang, H. H., J. Huang, K. Düvel, B. Boback, S. Wu, R. M. Squillace, C. Wu, and B. D. Manning. 2009. Insulin stimulates adipogenesis through the Akt-TSC2-mTORC1 pathway. PLoS One 4:e6189.